CHAPTER 5

Numerical Simulation of Rubber-assisted Forming Process

5.1 Introduction

Finite Element Method (FEM) is one of the versatile numerical technique used for solving physical problems posed in terms of differential or integral equations. In FEM modeling, the work-piece is represented by a collection of sub-domains called finite elements. The elements are bounded by sets of nodes. They define localized mass and stiffness properties of the model. Equations of equilibrium, in conjunction with applicable physical considerations such as compatibility and constitutive relations, are applied to each element to construct a system of equations. The system is then solved to find unknown values using advanced numerical techniques[89].

There are two modes of description of the deformations in continuous media, the Lagrangian and the Eulerian. The Lagrangian description employs the coordinates of a material point in the undeformed state as independent variables. The Eulerian description employs the coordinates of a material point in the deformed state. Because of this, the finite element mesh in the Eulerian system is spatially fixed, whereas in the Lagrangian system it moves with the material. The solution procedure is either explicit or implicit [89].

In the last few decades, the use of finite element for modeling the sheet metal hydro-forming process has increased tremendously. These simulations can predict the deformation process and the failure modes, such as wrinkling and local thinning, of the workpieces during sheet metal forming processes. In literature, both quasi-static implicit and dynamic explicit approach has been used for hydro-forming simulation.

In the static implicit methods, which were the very first methods used in simulation of metal forming processes, static equilibrium is satisfied in the unknown final configuration of a time increment. Also, inertia forces are neglected in implicit method. This method enables a full static solution of the deformation problem with convergence control. Theoretically the increment sizes can be very large; practically, however, it is limited by the contact conditions. Computational times increase almost quadratically with increasing element number. Because of the matrix inversion step and accurate integration schemes, memory requirements are also high. Another disadvantage of the implicit methods is said to be the problem of divergence of the solution. This is basically initiated due to the large number of contact nodes which can overload many implicit contact algorithms. Another disadvantage of the implicit methods is the singularity of the stiffness matrix at bifurcation points, such as instabilities at wrinkling initiation [90].

In comparison to implicit method, inertia forces are included in dynamic explicit method. Because of the quasi-static nature of most hydro-forming processes, the dynamic explicit approach has the advantage of less memory requirement and higher computational efficiency. The approach has several significant advantages over the conventional static implicit method for hydro-forming problems. In the explicit method, there is no direct, banded, linear equation solver. Consequently, the computational cost of a solution does not grow quadratically with the problem size. In general, the computational cost is linearly proportional to the problem size in the dynamic explicit procedure. Large deformation, and sliding and contact constraints, are relatively easy to implement in the explicit procedure. The kinematic contact constraints can be enforced explicitly by the direct trial-and-error method and, since there is no equation solver, change of contact conditions does not require the consideration of bandwidth optimization [91]. A by-product of the explicit scheme is the determination of the wrinkles. The wrinkles are initiated through numerical inaccuracies. Usually, the region of the wrinkles is quite accurately determined; but the number of wrinkles and the amplitude of the wrinkles may be inaccurate due to the numerically driven initiation process.

The explicit character of the numerical scheme is fulfilled if and only if the mass

matrix is lumped, i.e. is diagonal. Furthermore, the speed advantages can be hold only if the element computations are as few as possible. This is maintained by using single-quadrature elements, which deliver rather poor stress and strain accuracy. It is claimed that the error introduced by a lumped mass matrix is compensated by the reduced integration schemes of the elements. However, this leads to the disadvantages that local stresses and spring-back is not reliably computed [91]. Another drawback of dynamic explicit approach is that it is conditionally stable. The stability limit for the explicit integration operator is that the maximum time increment must be less than a critical value of the smallest transition times for a dilatational wave to cross any element in the mesh. Also, the nature of the explicit method limits it to the analysis of short transient problems. Thus, if this approach is used for quasi-static problems, the inertia effects or dynamic effects must be small enough to be neglected. However, that requires very small time increments and it leads to a large amount of computational time. Therefore, to solve quasi-static problems, it is conventional to convert the real problem to a virtual problem with a different mass density and processing time by means of mass and time scaling [90].

In the present work, dynamic explicit approach has been used for simulating the sheet hydro-forming process in ABAQUS/explicit.

5.2 Simulation for Stainless Steel 304 Cup using FEA

Finite element simulation for stainless steel 304 cup is carried out in finite element code ABAQUS-explicit. The simulation is carried out for both conventional, and rubber assisted deep drawing. The Detailed description of the code and its application are explained in ABAQUS manual [42].The components design in ABAQUS/CAE is treated as the shell. The punch, die & blank holder is assumed to be rigid while rubber and sheet are deformable. Both elastic and plastic material properties are given in the definition of Material Model. The Actual stress-strain curve is used for modeling of rubber material during rubber assisted deep drawing process which is best suitable for 'Marlow Material Model' [92] of rubber. The section thickness 0.8mm for stainless steel and 3mm for rubber is used. Here dy-

namic explicit analysis is carried out to get accurate results in minimum simulation time [89].

The blank is meshed with conventional shell element 'S4R'. The element S4R is a 4-node, quadrilateral stress/displacement shell element with reduced integration and a large strain formulation. This element allows transverse shear deformations. It uses reduced integration to avoid shear and membrane locking. As tool components are assumed to be rigid therefore rigid element 'R3D4' has been used for their discretization. Element R3D4 uses a 3-D, 4-node bilinear quadrilateral rigid element. The dimensions of the blank elements should be uniform since the minimum size in the elements determines the step size of the calculation. Contact is modeled between the components in both conventional, and rubber assisted deep drawing. Due to tangential behavior (Coulomb assumption) between the blank and blank holder, the friction coefficient of 0.15 has been used for steel blanks. Penalty based approach of contact, where the friction effects are described via the Coulomb law [93], is used for both conventional and rubber assisted deep drawing. Symmetric boundary conditions are applied on the nodes lying at the symmetric planes. The die and holder are completely constrained in both processes. The die block is also constrained in cases of rubber assisted deep drawing. Symmetrical boundary conditions are specified on the appropriate edges of the blank and rubber. Punch is constrained in other directions except for axial direction. The velocity of 1000 mm/min is provided to punch in the axial direction for both processes. The FE model of conventional deep drawing and rubber assisted deep drawing are shown in figure 5.1 and figure 5.2 respectively.

Result And Discussion

The numerical results are evaluated for conventional and rubber assisted, deep drawing process using the finite element technique. The blank material used for the numerical simulation is stainless steel 304 of 0.8mm thickness. For rubber assisted deep drawing process thin natural rubber 3mm thickness is used. The experimental results, the variation of thickness along the cup wall, variation of Von-Mises and maximum principal stress is studied and compared for both conventional and rubber assisted deep drawing process.

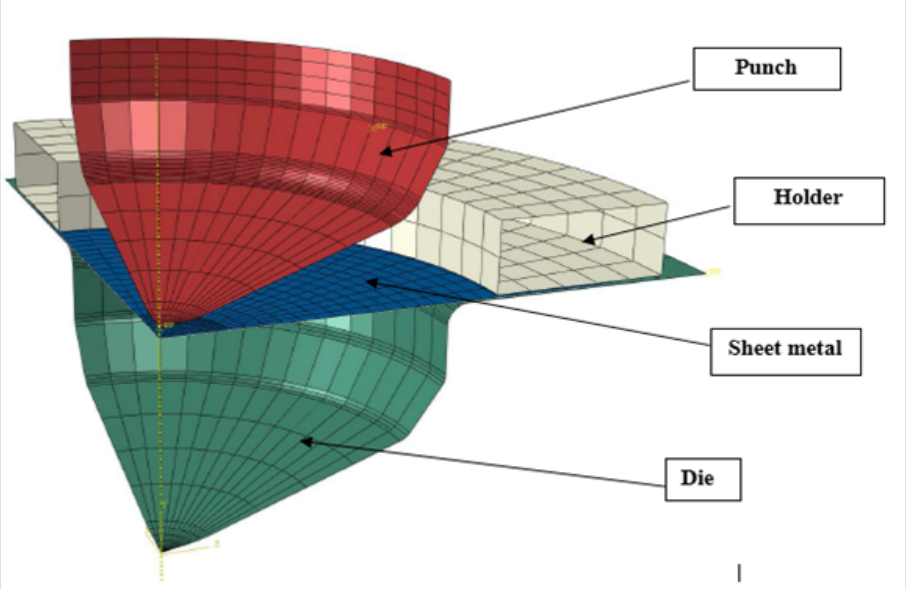

Figure 5.1: Finite element model of Conventional Deep Drawing

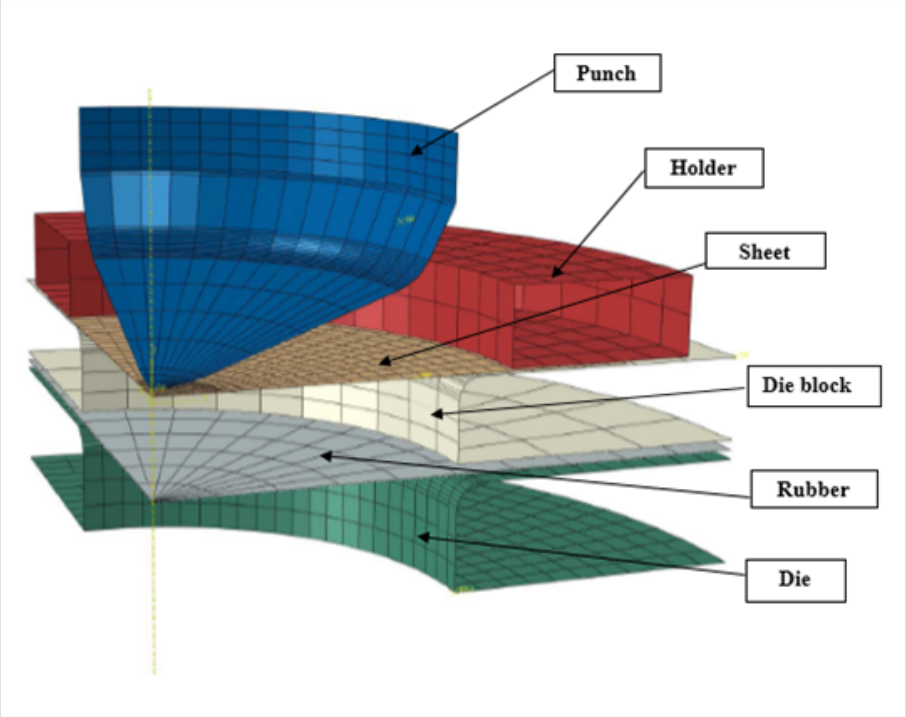

Figure 5.2: Finite element model of Rubber assisted deep drawing

Experiment Results The stainless steel SS-304 Cup with thickness 0.8mm formed by conventional deep drawing and rubber assisted deep drawing as shown in figure 5.3 and figure 5.4.

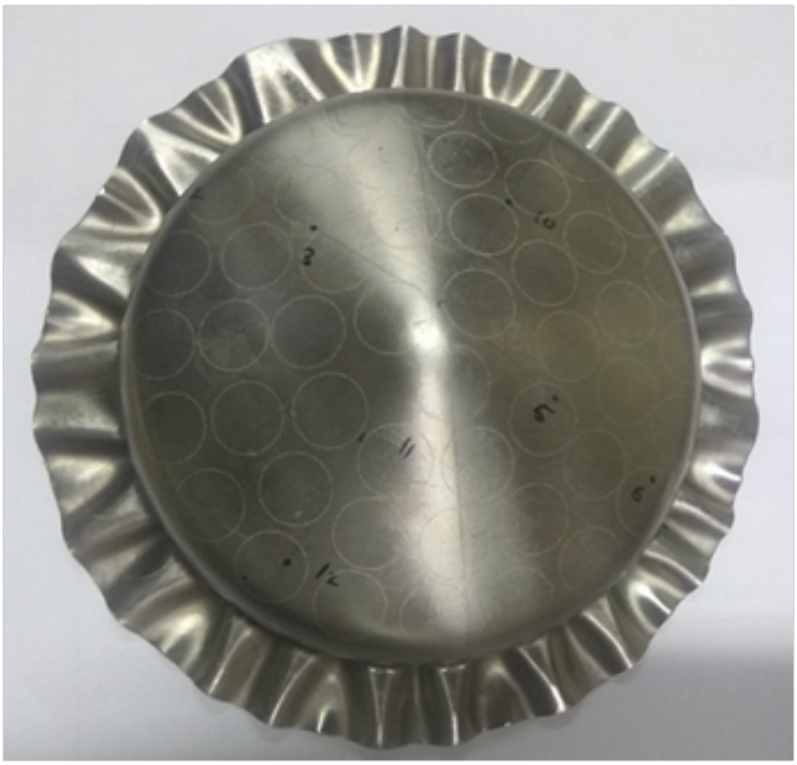

Figure 5.3: Component formed by conventional deep drawing

Thickness analysis The numerical simulation is carried out and compared for conventional and rubber assisted forming process. The corresponding thickness variation is shown in (Figure 5.5 and 5.6) respectively. The thickness variation along the cup wall is studied for the same punch velocity. Equal reduction in thickness is observed for both the processes. The thickness build-up (0.867mm) near holder region is also same for both processes. The comparative plot of thickness variation for both the processes is shown in figure 5.7. In the numerical simulation of conventional and rubber assisted forming, the Von-Mises stress distribution and Plastic strain are studied From the Figure 5.10, it can be inferred that von-Mises stress distribution between center of the cup to the 40 mm radial distance is almost uniform and varies between 590 MPa to 400 MPa. Whereas, in conventional deep drawing, it varies between 620 MPa to 350 MPa. Hence, rubber helps in more uniform distribution of stress during forming. This has been further substantiated by comparing statistical

Figure 5.4: Component formed by rubber assisted deep drawing

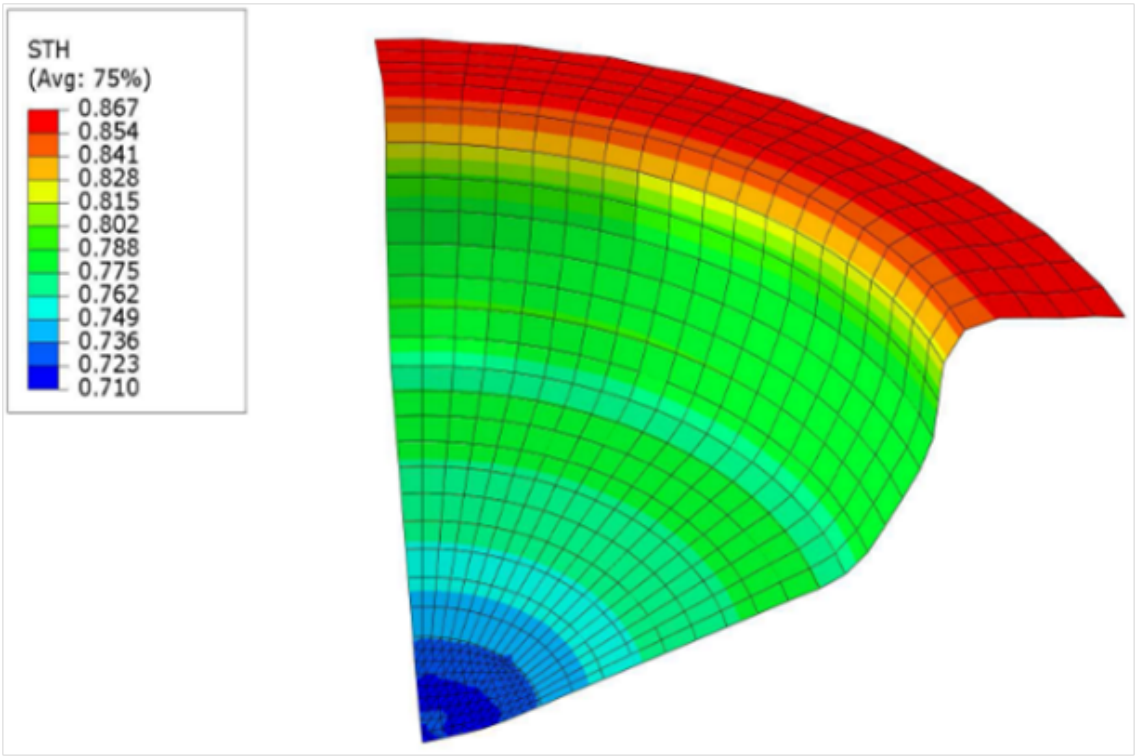

Figure 5.5: Thickness distribution in conventional deep drawing

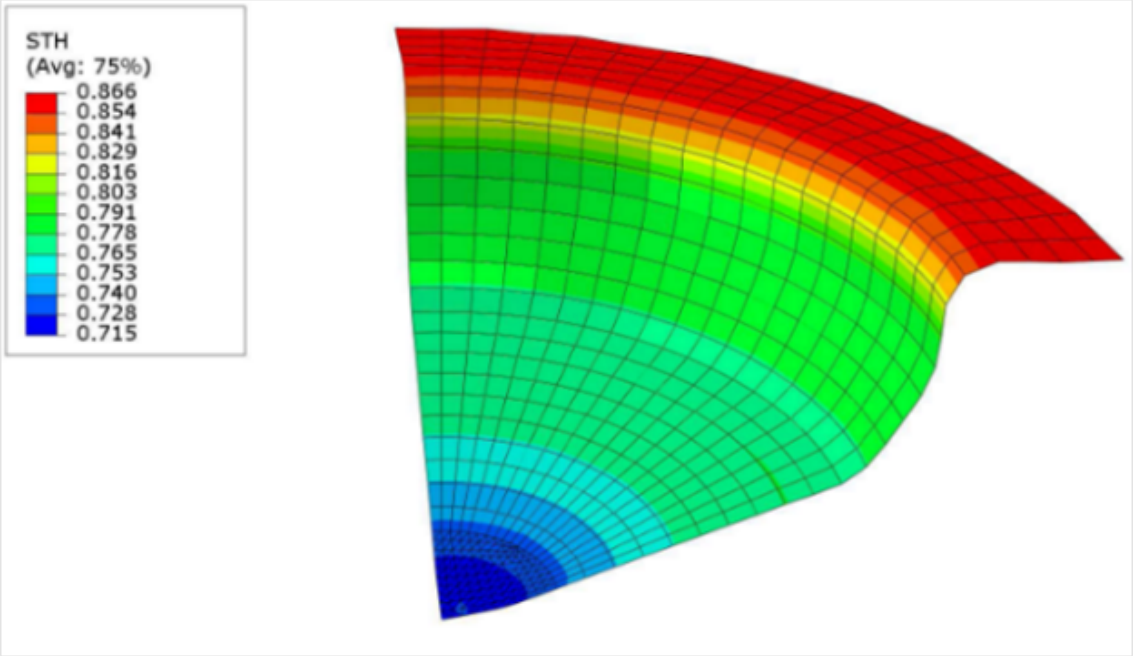

Figure 5.6: Thickness distribution in rubber assisted deep drawing

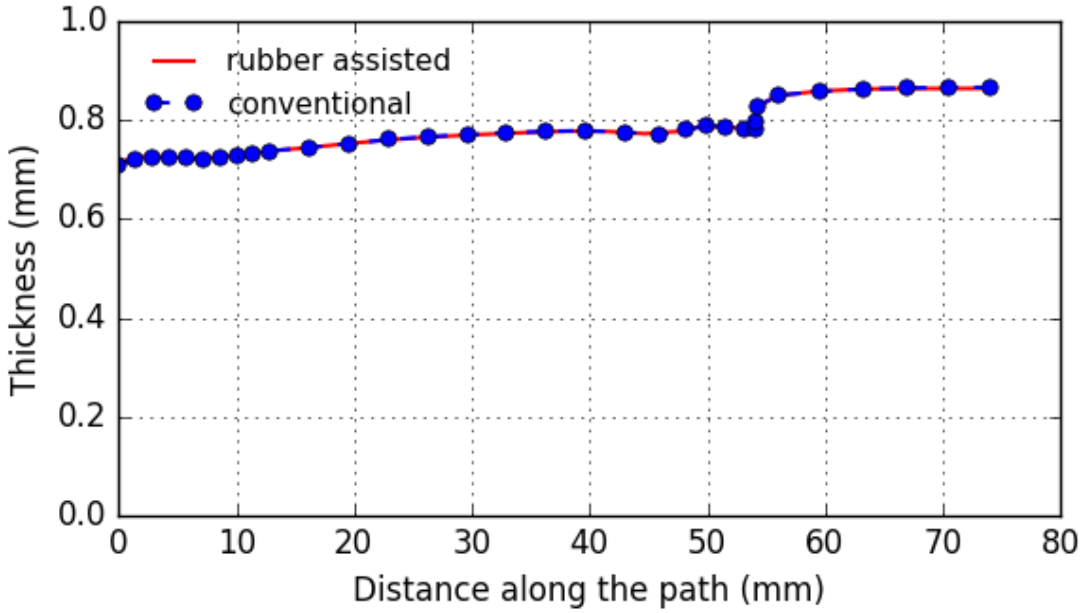

Figure 5.7: Thickness distribution along the distance from cup centre in rubber assisted deep drawing

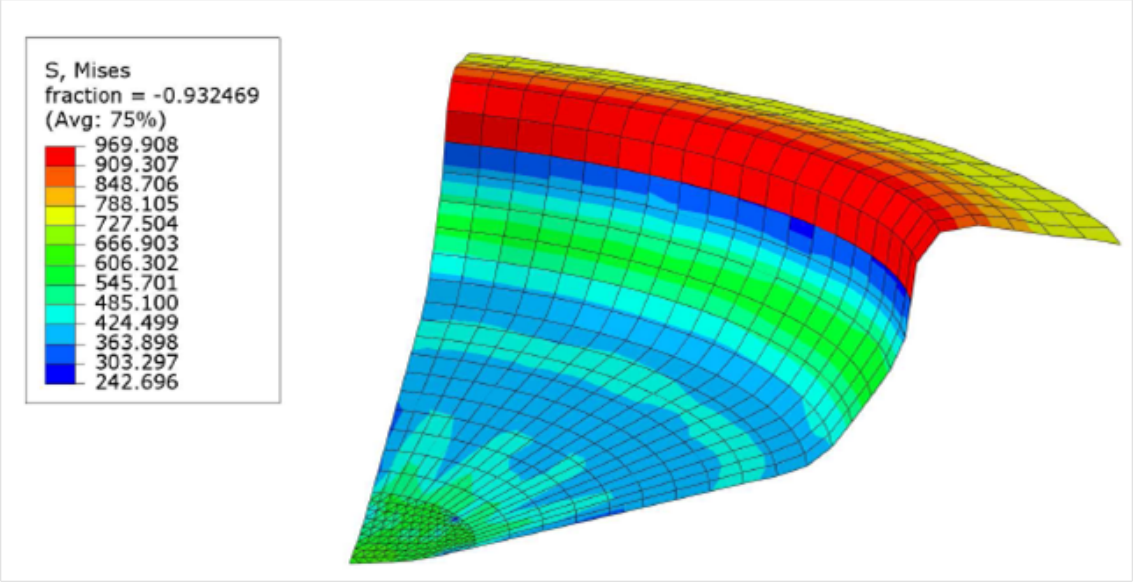

Figure 5.8: Von-Mises stress in conventional deep drawing

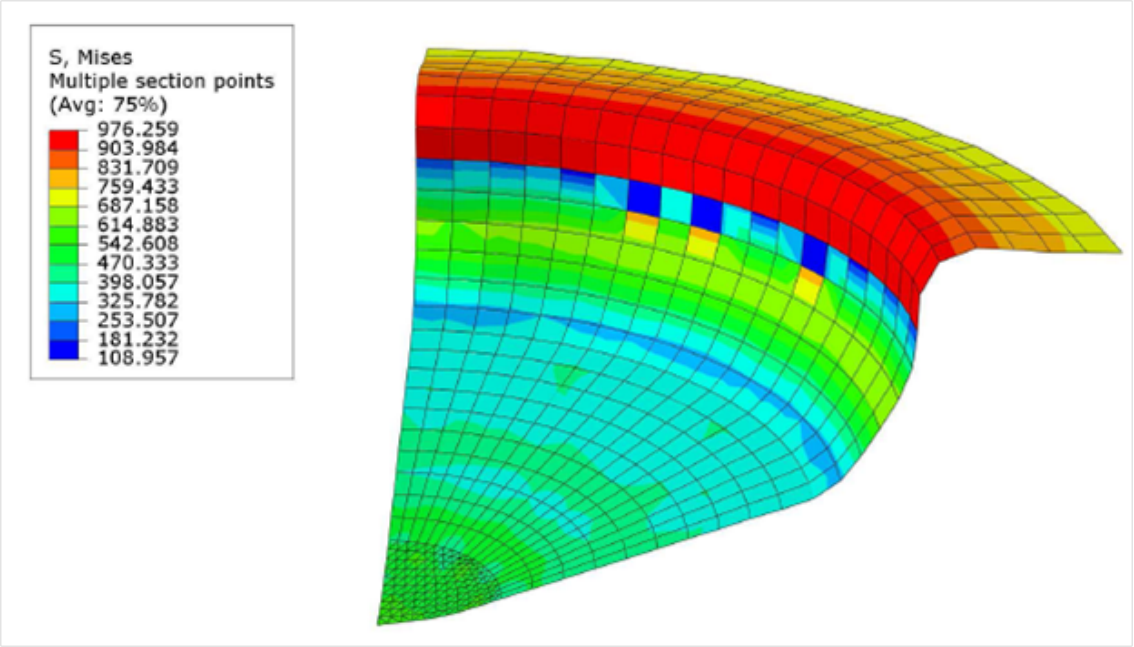

Figure 5.9: Von-Mises stress in Rubber assisted deep drawing

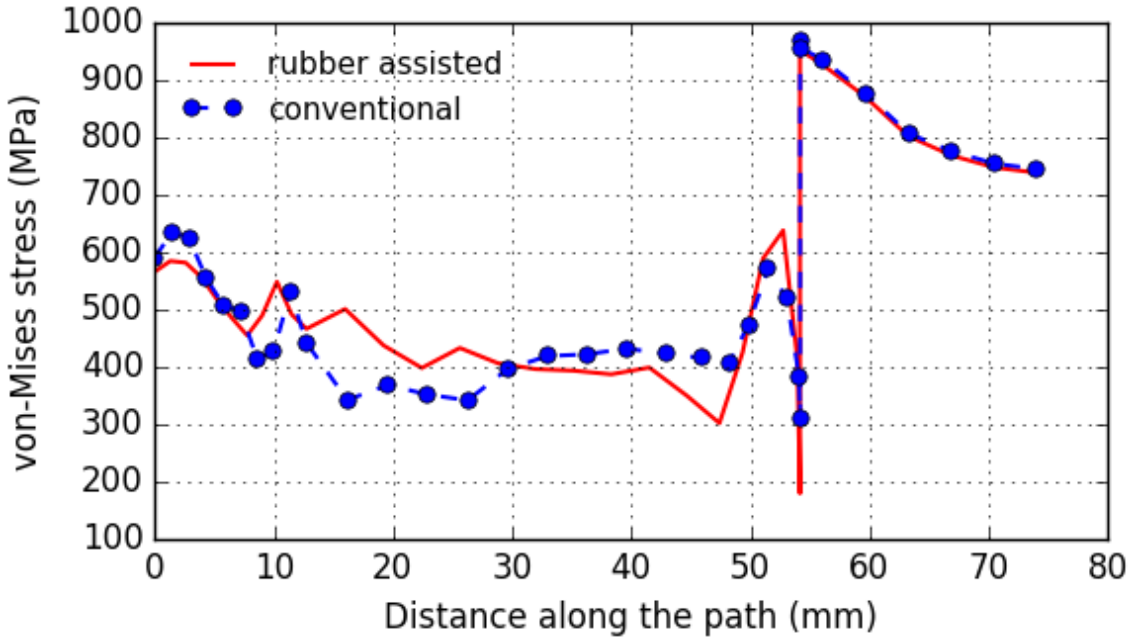

Figure 5.10: Von-Mises stress comparison

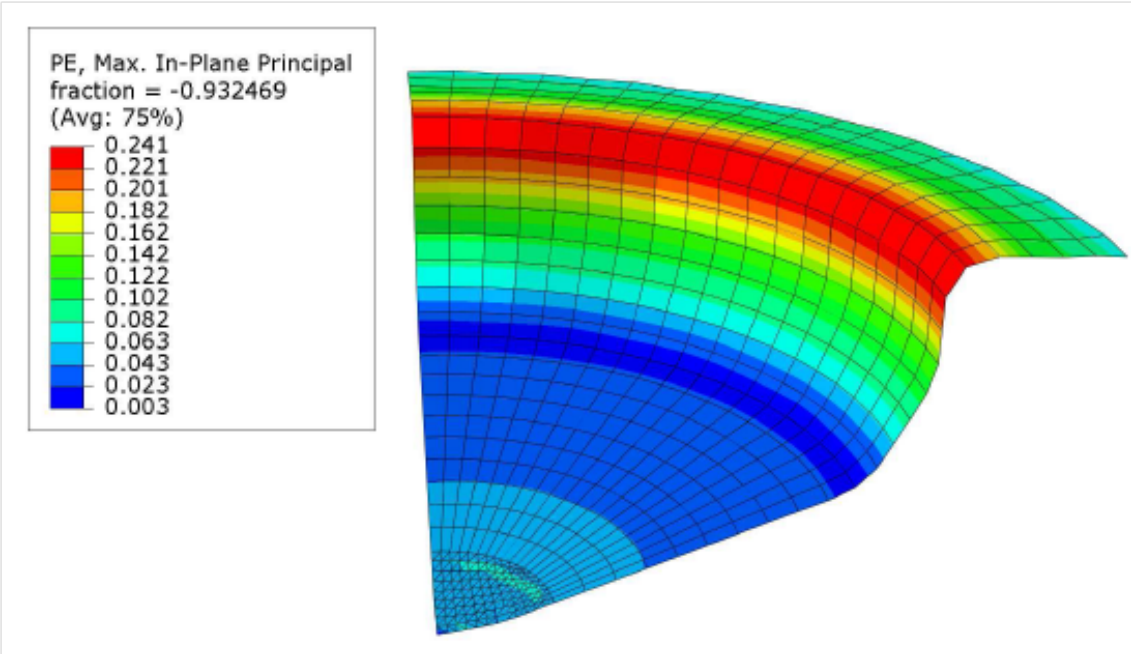

Figure 5.11: Plastic strain in conventional deep drawing

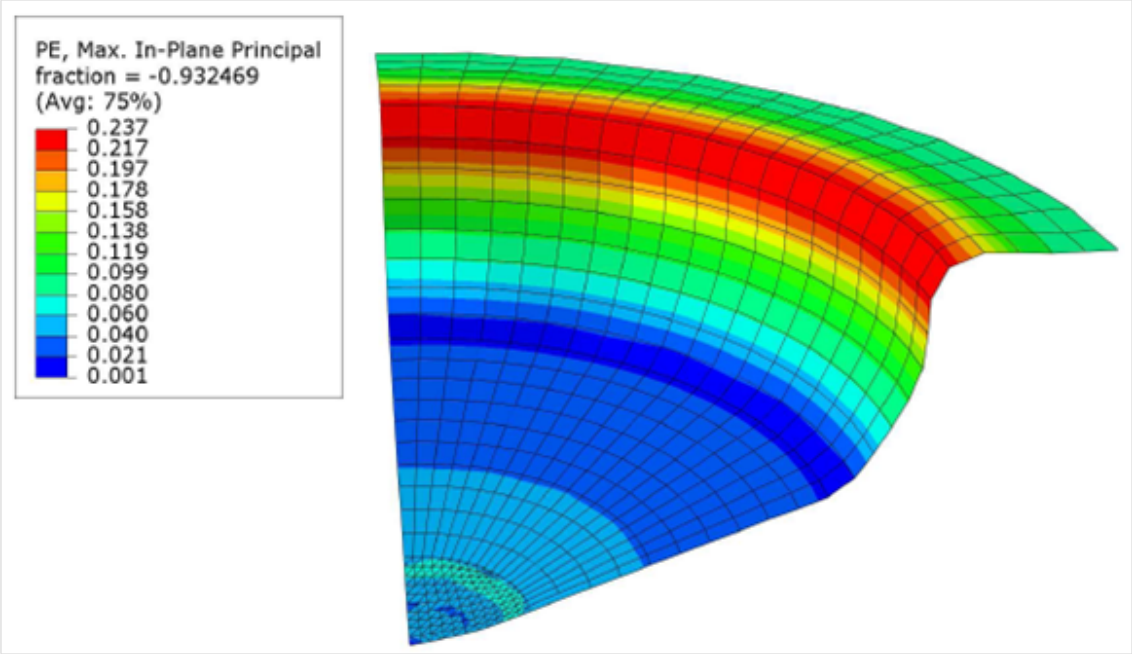

Figure 5.12: Plastic strain in Rubber assisted deep drawing

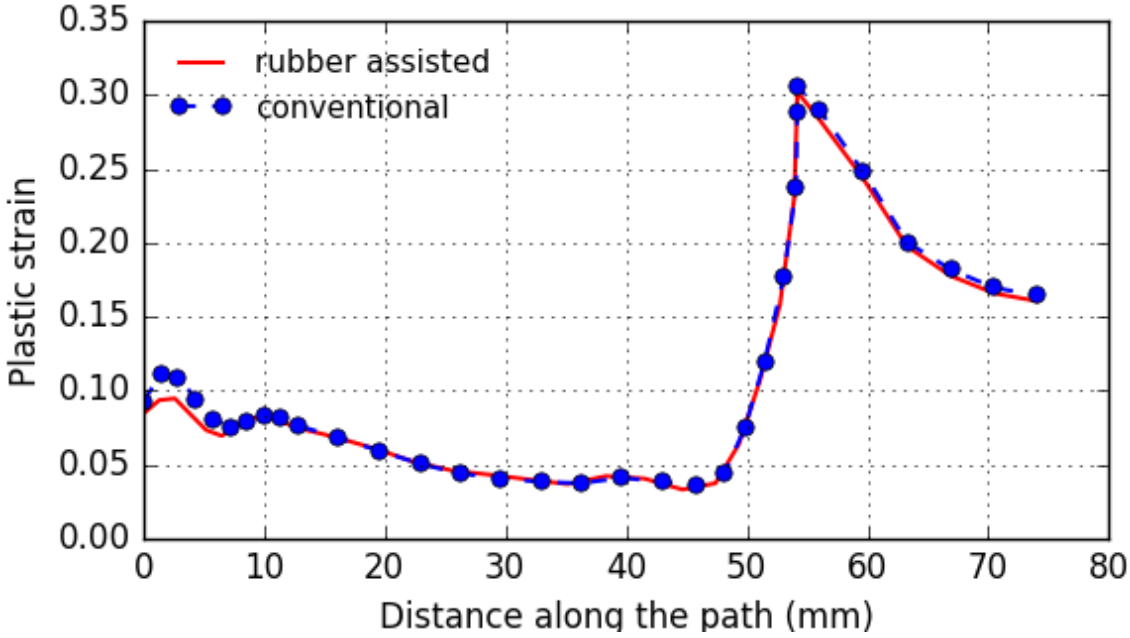

Figure 5.13: Comparative plot for Plastic strain

parameters of the von-Mises stress distribution. The mean von-Mises stress values for conventional and rubber-assisted forming process are 457 MPa and 475 MPa respectively. However, the standard deviation for corresponding processes are 90 MPa and 68 MPa respectively.

As shown in figure 5.13, the plastic strain is almost same for both the cases. The minimum thickness obtained in simulation is 0.7 mm which matches with experimental results.

5.3 Simulation of Copper Cone using FEA

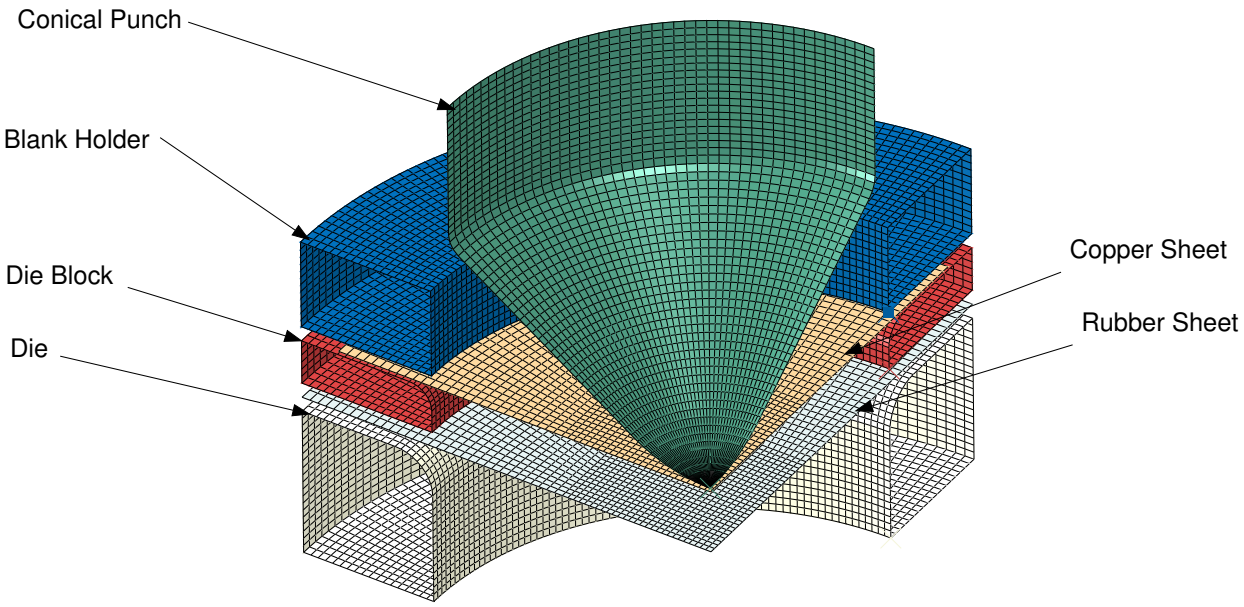

Figure 5.14: Finite element model of Rubber assisted Deep Drawing Operation

Finite element simulation of sheet hydro-forming process, for conical cups made of copper, has been carried out in finite element code ABAQUS-explicit. The simulation has been carried out for both conventional and rubber assisted hydro-forming process. The FE modeling procedure is same as discussed in section 5.2. The mesh details for this case is shown in table 5.1. The dimensions of the blank elements

Table 5.1: Mesh details

Component	**Element Type**	**No. of Elements**	**No. of Nodes**
Sheet	S4R	1976	2054
Die Block	R3D4	5175	5244
Holder	R3D4	1444	1482
Punch	R3D4	1760	1840
Riser	R3D4	1430	1485

should be as uniform as possible, as the minimum size in the elements determine the step size of the calculation. Contact was modeled between the blank and the punch, between the blank and the die surface, and between the blank and the blank holder, using the Coulomb assumption. A uniform pressure load was applied directly to the blank. The friction coefficient between the blank and punch was assumed as 0.15

for copper blanks and 0.15 for steel blanks, which was helpful for the success of the process: and that between the blank and the blank holder could be assumed to be much lower than that between the blank and the punch because of the lubricants used.

5.3.1 Loads and Boundary conditions

Symmetric boundary conditions have been applied on the nodes lying at the symmetric planes. The die, die block and holder have assumed to be rigid and have been completely constrained. Except axial direction, punch have been constrained in other directions. The punch have been given velocity of 200 mm/min in axial direction. The loads and boundary conditions are shown in figure 5.15.

Contact (Penalty-based approach) assuming Coulomb friction between the blank and the punch, between the blank and the die surface, and between the blank and the blank holder was modeled. Friction between the blank and the die surface was very low (friction coefficient 0.05 or lower) due to the fluid pressure. Higher friction (friction coefficient 0.08) was assumed between the blank edge (about 10 mm in radial direction) and the die surface, where the contacting condition was highly changed due to the severe thickening and lower fluid pressure. The friction coefficient between the blank and the punch was assumed to be 0.15; between the blank and the blank holder the friction was assumed to be much lower than that between the blank and the punch because of the lubricant used between the blank and the blank holder. Symmetrical boundary conditions were specified on the appropriate edges of the blank. The liquid was not modeled; instead a uniform distribution pressure within the die opening was used to apply the fluid pressure directly on the blank, while the fluid pressure was assumed to be linearly lowered in the radial direction under the blank flange, until it was zero at the edge of the blank. The pressure distribution was assumed to vary with the punch travel along the flange area.

5.3.2 Validation of Numerical Model

The finite element model has been validated for the conventional sheet hydroforming process experimentally. The thickness variation and deformed shape as

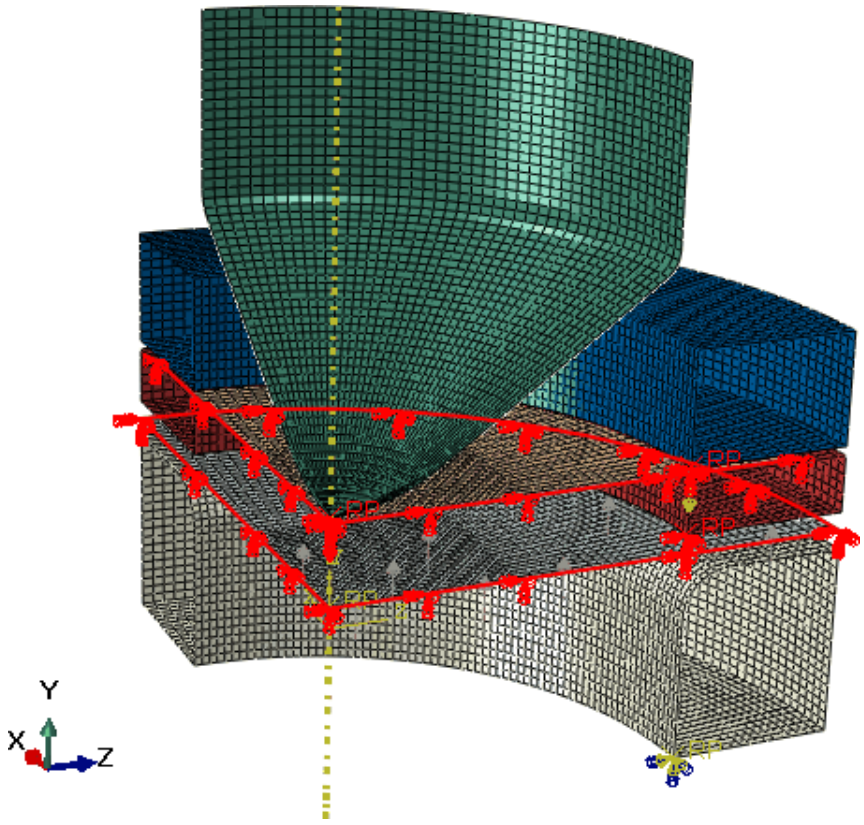

Figure 5.15: Loads and boundary conditions for sheet hydro-forming process

obtained from the finite element analysis have been compared with that obtained from sheet hydro-forming experiment. The FE model has been validated for copper blank with conical die (84^o).

5.3.3 Results and Discussion

The numerical results are evaluated for conventional, rubber assisted and rubber assisted hydro-forming process using the finite element technique for making conical cup shape. The blank material used for the numerical simulation is pure copper sheet of 0.9 mm thickness. For rubber assisted and rubber assisted hydro-forming process, thin rubber sheet (4 mm thick) made of natural rubber have been used. If the cone angle is more, the forming operation can be carried out in single step without failure. However, if the cone angle of the final product is small, the forming operation is carried out in different stages, wherein the cone angle of the punch varies in steps. This way the cup with smaller cone angle is realized without fracture. The variation of thickness along the cup wall with cone angle has been studied for the different forming processes mentioned above. The variation of von-Mises stress and

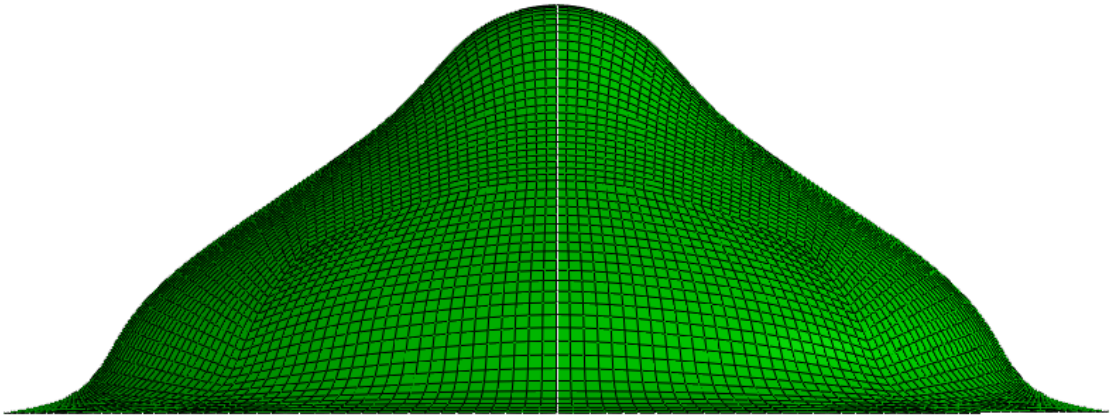

(a) FE Simulation

(b) Experiment (half)

Figure 5.16: Model validation: Deformed shape

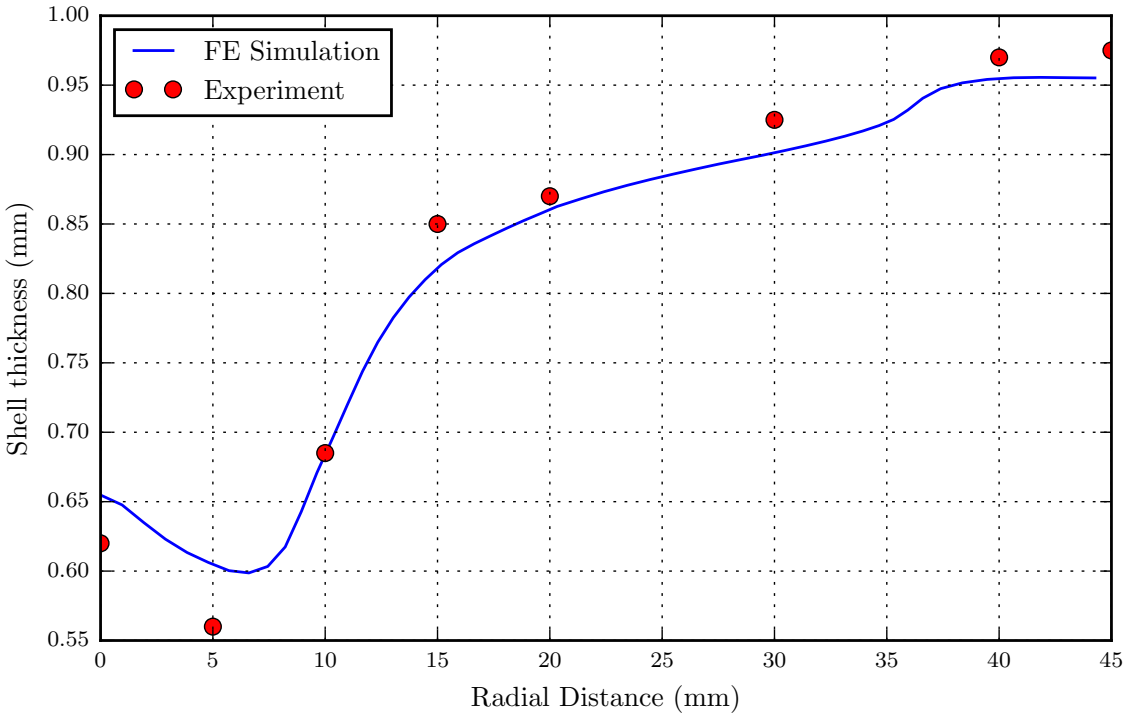

Figure 5.17: Comparison of shell thickness

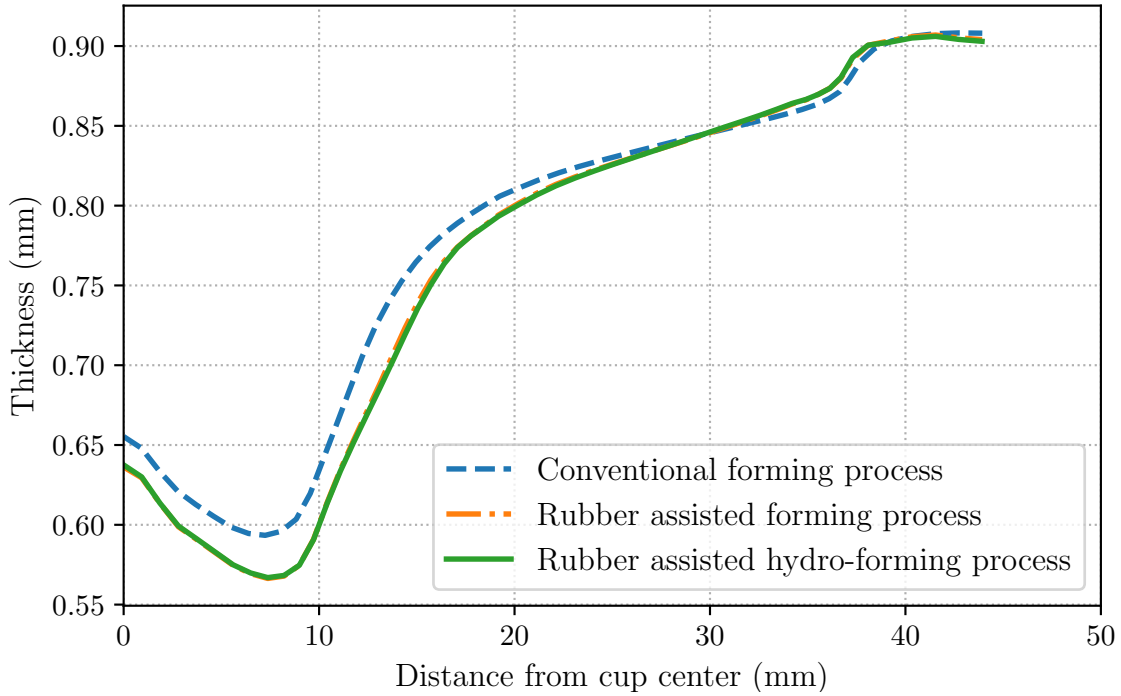

Figure 5.18: Variation of thickness along cone wall for cone angle 84^o

maximum principal stress has also been studied. The axial deformation of the cup for different cone angle has also been presented.

Thickness variation along the cup wall for different forming processes

The numerical simulations have been carried out for different forming processes viz. conventional forming process, rubber assisted forming process and rubber assisted hydro-forming process for cone angle of 84^o. The thickness variation along the cup wall is shown in figure 5.18. It has been observed that for the same punch velocity higher thickness reduction is achieved for rubber assisted forming processes. Also, the thickness variation along the wall for rubber assisted forming process and rubber assisted hydro-forming process is benign for conical cup made of copper sheet. The thickness build-up near holder region is reduced in rubber assisted forming processes.

Study of thickness variation along the cup wall with cone angle

For the conventional forming process, the thickness variation along the cup wall with varying cone angle is shown in figure 5.19. It can be observed from the graph that with the increase in the cone angle the thickness near to center of the cone

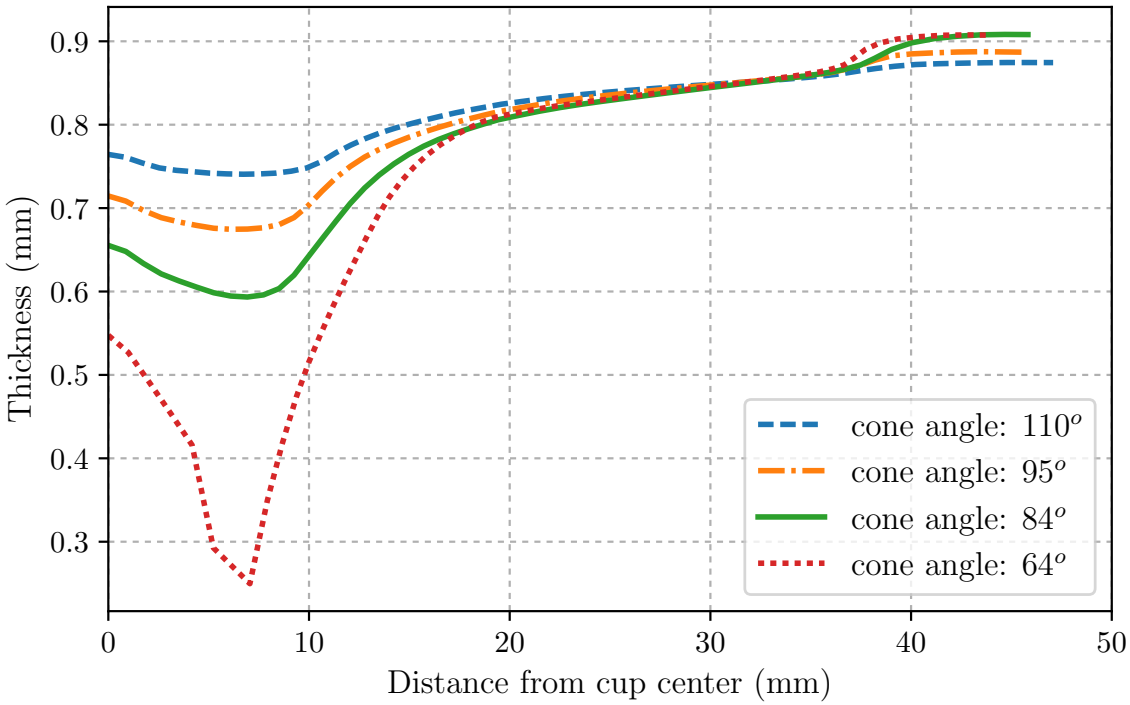

Figure 5.19: Variation of thickness along cup wall for different cone angle (conventional sheet forming process)

decrease, and after a critical cone angle sheet fractures. Also, there is a increase in thickness built-up, near to holder region, with the decrease in cone angle. The thickness variation along the cup wall with varying cone angle for rubber assisted sheet forming process is shown in figure 5.20. Similar to conventional process, in this case also thickness decreases with the decrease in cone angle. Thickness build-up near the holder region increases initially with the decrease in cone angle, but at lower cone angles the thickness built-up does not change. As shown in plot, for the cone angle of 64^o, the thickness variation near to center is not continuous. This is due to large plastic deformation causing fracture in this region. The thickness variation along the cup wall with varying cone angle for rubber assisted sheet hydro-forming process is shown in figure 5.21. The thickness variation for this case is very similar to rubber assisted forming process. In this case also, at smaller cone angle fracture near to center of the cup occurs. This is evident with the large thickness variation at the cup central region.

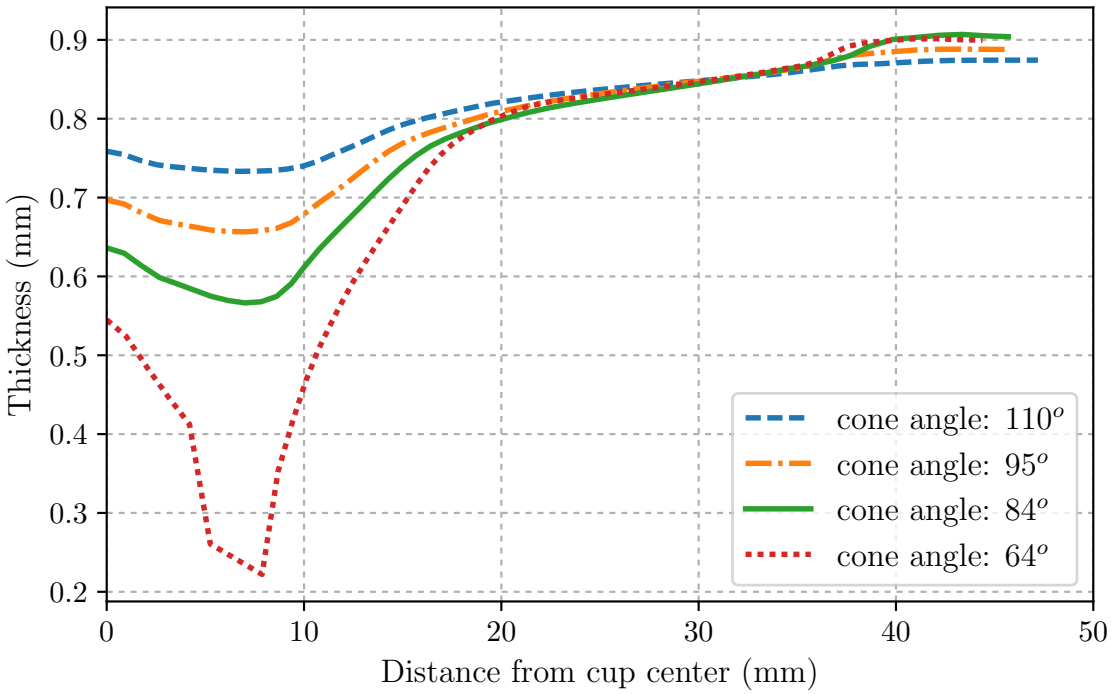

Figure 5.20: Variation of thickness along cup wall for different cone angle (rubber assisted sheet forming process)

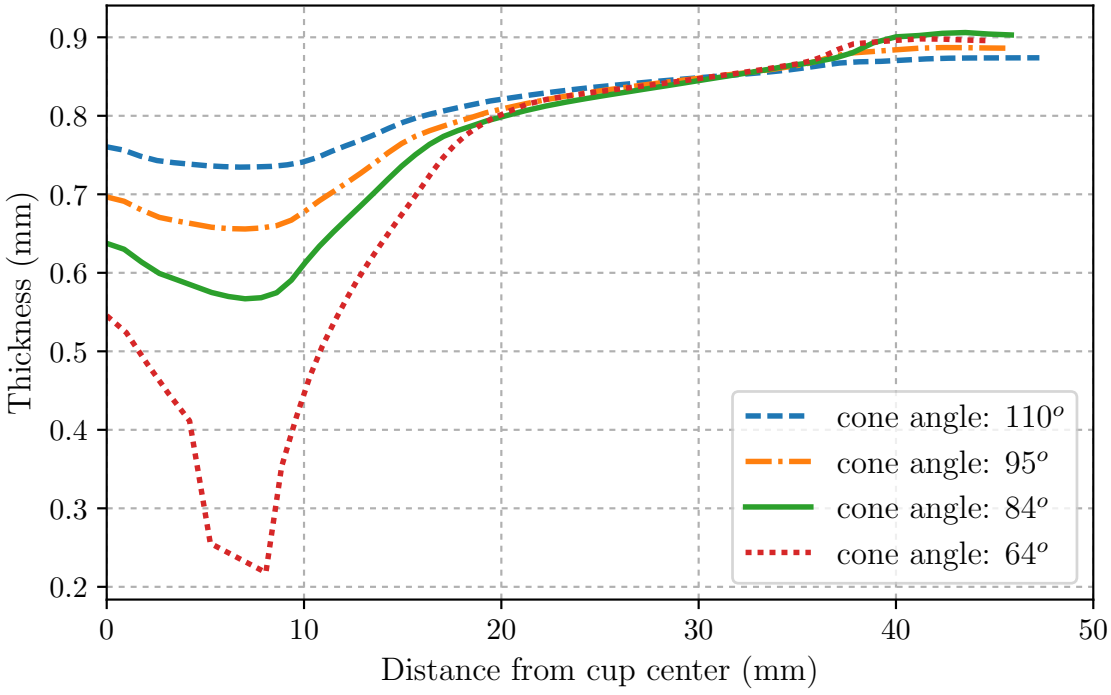

Figure 5.21: Variation of thickness along cup wall for different cone angle (rubber assisted sheet hydro forming process)

Effect of cone angle on von-Mises stress distribution in conical cup

The von-Mises stress distribution for different cone angles corresponding to conventional, rubber assisted and rubber assisted hydro-forming process are shown in figure 5.22, figure 5.23 and figure 5.24 respectively. The radial stress in drawing operation is directly proportional to the logarithmic ratio of blank diameter to cup diameter [87]. Thus, with the decrease in cone angle, cup diameter decreases which in turns increases the radial stress. Similar pattern of stress variation has been captured in FE simulation for all the forming process i.e the von-Mises stress in the formed cup increases with the decrease in cone angle.

With the decrease in cone angle, the maximum von-Mises stress location shifts towards the center region. In comparison to conventional forming process, the von-Mises stress in the cup is more in rubber assisted forming/ hydro-forming process. The difference in maximum von-Mises stress in rubber assisted forming process and rubber assisted hydro-forming process is less. The high von-Mises stresses in the cup central region corresponding to 64^o cone angle shows fracture in the cup. In the rubber assisted hydro-forming process, the spread of maximum stresses is localized as compared to rubber assisted forming process.

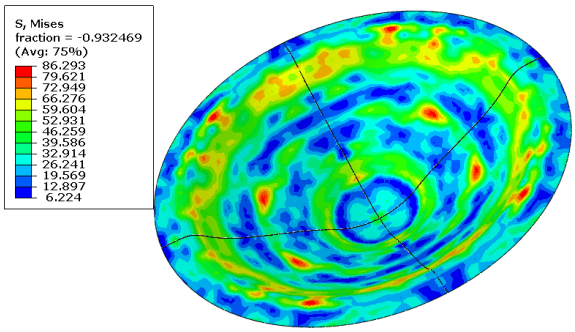

(a) Cone angle: 110^o

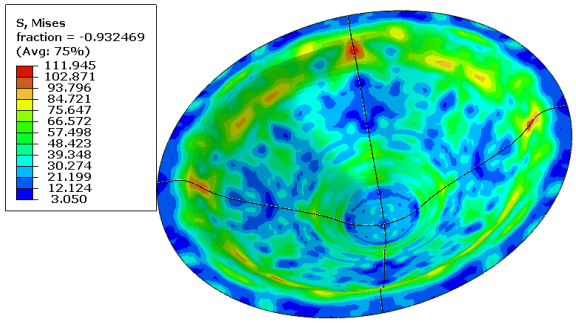

(b) Cone angle: 95^o

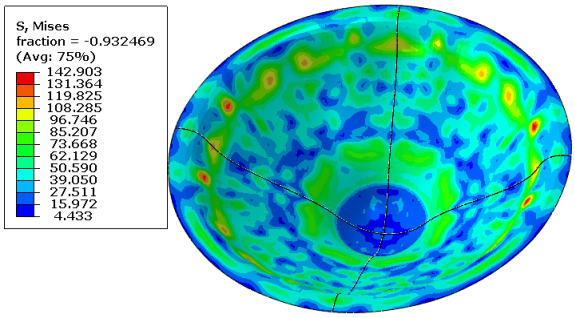

(c) Cone angle: 84^o

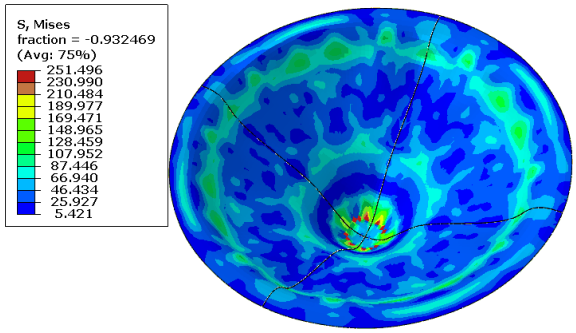

(d) Cone angle: 64^o

Figure 5.22: Variation of von-Mises stresses with cup cone angle [Conventional forming process]

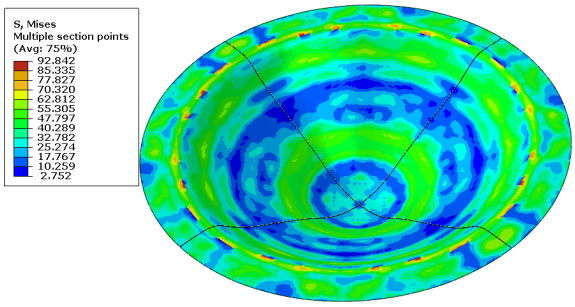

(a) Cone angle: 110^o

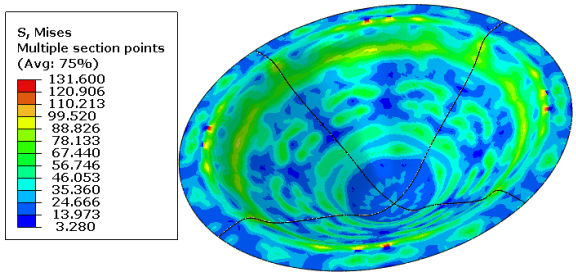

(b) Cone angle: 95^o

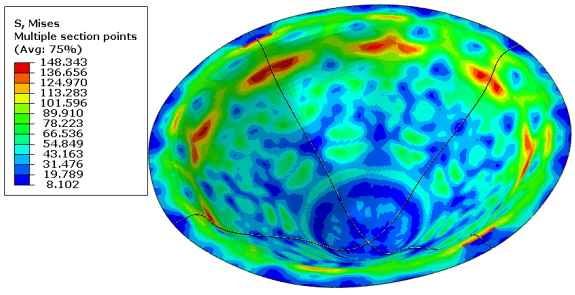

(c) Cone angle: 84^o

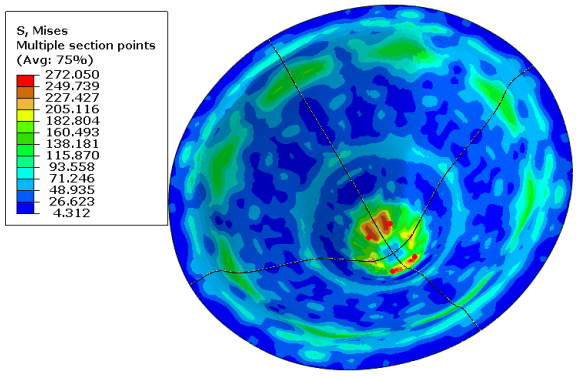

(d) Cone angle: 64^o

Figure 5.23: Variation of von-Mises stresses with cup cone angle [Rubber assisted forming process]

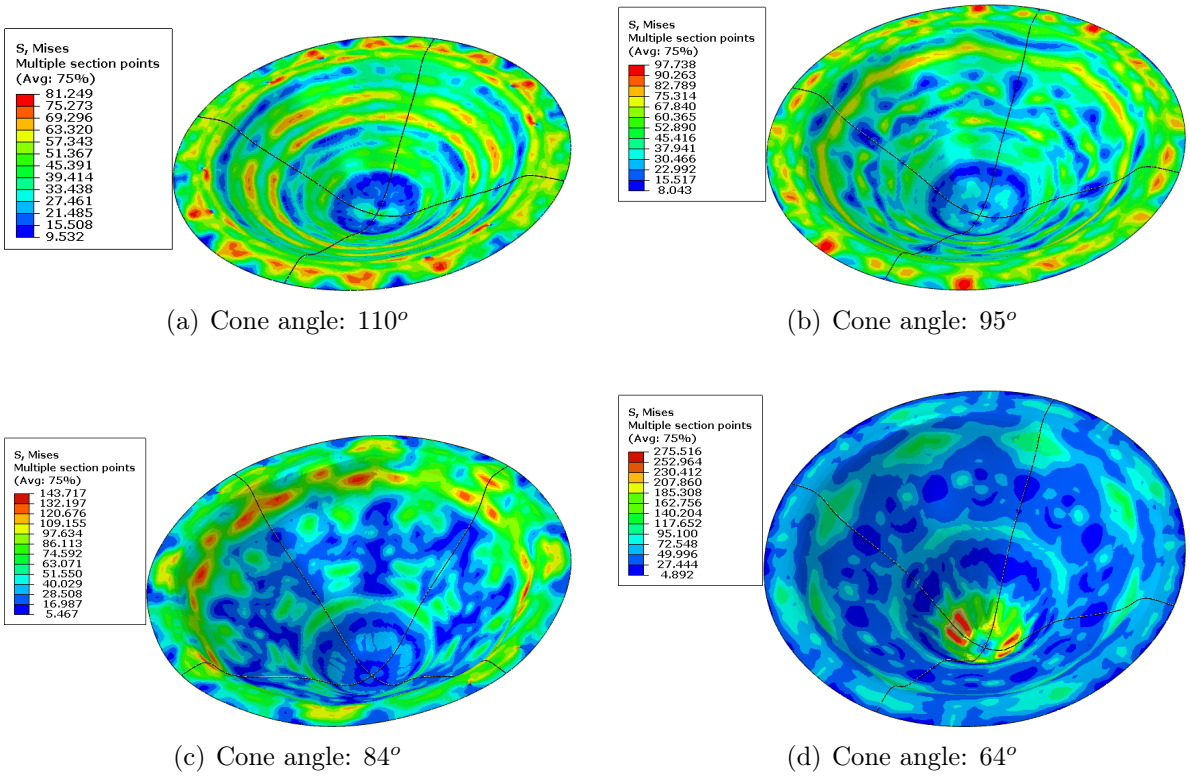

(a) Cone angle: 110^o

(b) Cone angle: 95^o

(c) Cone angle: 84^o

(d) Cone angle: 64^o

Figure 5.24: Variation of von-Mises stresses with cup cone angle [Rubber assisted hydroforming process]

5.4 Simulation of Hemispherical Copper Cup using FEA

Finite element simulation of sheet hydro-forming process, for cups made of copper, has been carried out in finite element code ABAQUS-explicit. The FE modeling procedure is same as discussed in section 5.2.

5.4.1 Plasticity Model and Boundary Conditions

Pure copper with blank thickness 2mm and natural rubber with 3mm thickness are used for this study. In general power law is adopted for modelling the plasticity of stress strain curve of the material. In this study nonlinear properties are considered for modelling of true stress-strain curve from the tensile test. Marlow model of rubber is used for modelling because rubber is a hyper elastic material. The advantage of using this plasticity model is the tested stress strain curve is considered into the simulation.

Symmetric boundary conditions have been applied on the nodes lying at the symmetric planes. The die, die block and holder have assumed to be rigid and have been completely constrained. Except axial direction, punch have been constrained in other directions. The punch have been given velocity of 1000 mm/min in axial direction. Contact (Penalty-based approach) is modeled assuming Coulomb friction between the blank and the punch, between the blank and the die surface, and between the blank and the blank holder. Friction between the blank and the die surface was very low (friction coefficient 0.05 or lower) due to the fluid pressure. Higher friction (friction coefficient 0.08) is assumed between the blank edge (about 10 mm in radial direction) and the die surface, where the contact condition is severe due to the thickening and lower fluid pressure. The friction coefficient between blank and punch is assumed to be 0.15; between blank and blank holder the friction was assumed to be much lower than that between the blank and the punch because of the lubricant used between blank and blank holder. Symmetrical boundary conditions were specified on the appropriate edges of the blank. The liquid was not modeled; instead a uniform distribution pressure within the die opening was used to apply

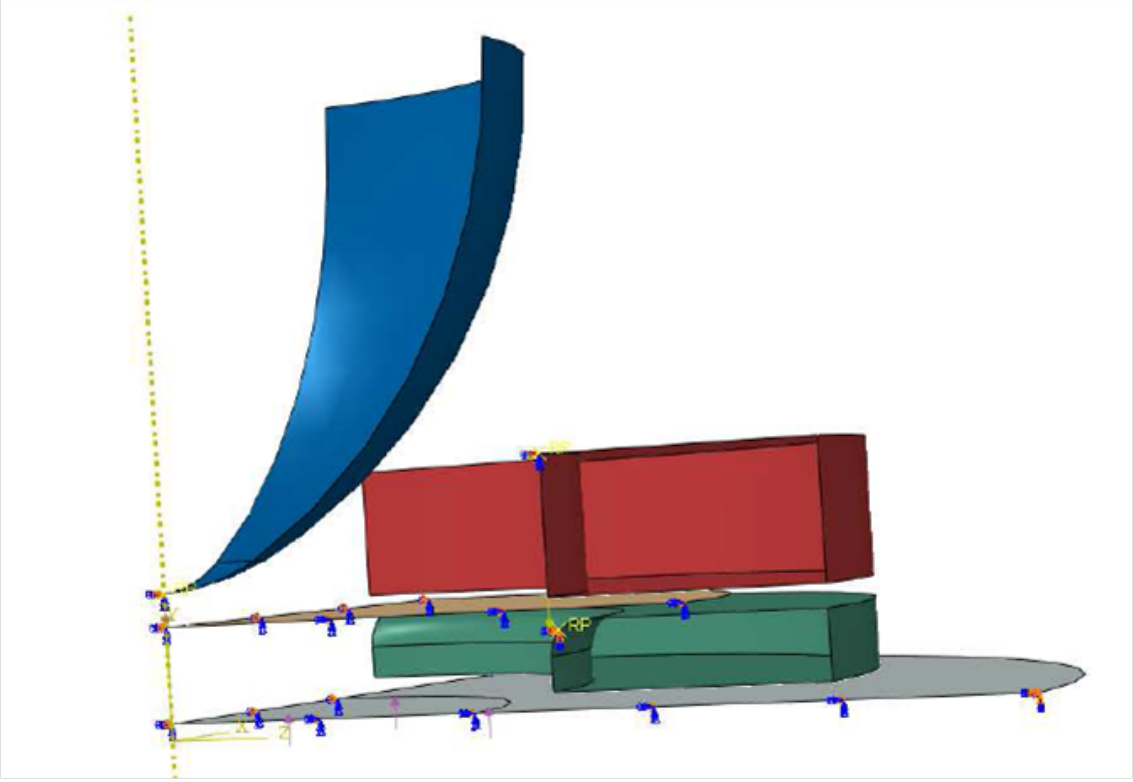

Figure 5.25: Assembly of rubber assisted sheet Hydro-forming

the fluid pressure directly on the blank, while the fluid pressure was assumed to be linearly lowered in the radial direction under the blank flange, until it was zero at the edge of the blank. The pressure distribution was assumed to vary with the punch travel along the flange area. The FEM model is shown in figure 5.25.

5.4.2 Validation of Numerical Model

The finite element model has been validated for the rubber assisted sheet Hydro-forming process experimentally. The thickness variation and deformed shape as obtained from the finite element analysis has been compared with the obtained from experiment.

In order to study the introduction of fluid pressure in rubber assisted Hydro-forming process. Finite element simulation have been carried out for hemispherical cup with fluid pressure. The thickness variation along the cup wall by an applying fluid pressure is shown in figure 5.29. The von-Mises stresses, the maximum principal stresses and axial deformation decreases in rubber assisted forming due to fluid pressure. The von-Mises stresses distribution, the max principal stress distribution

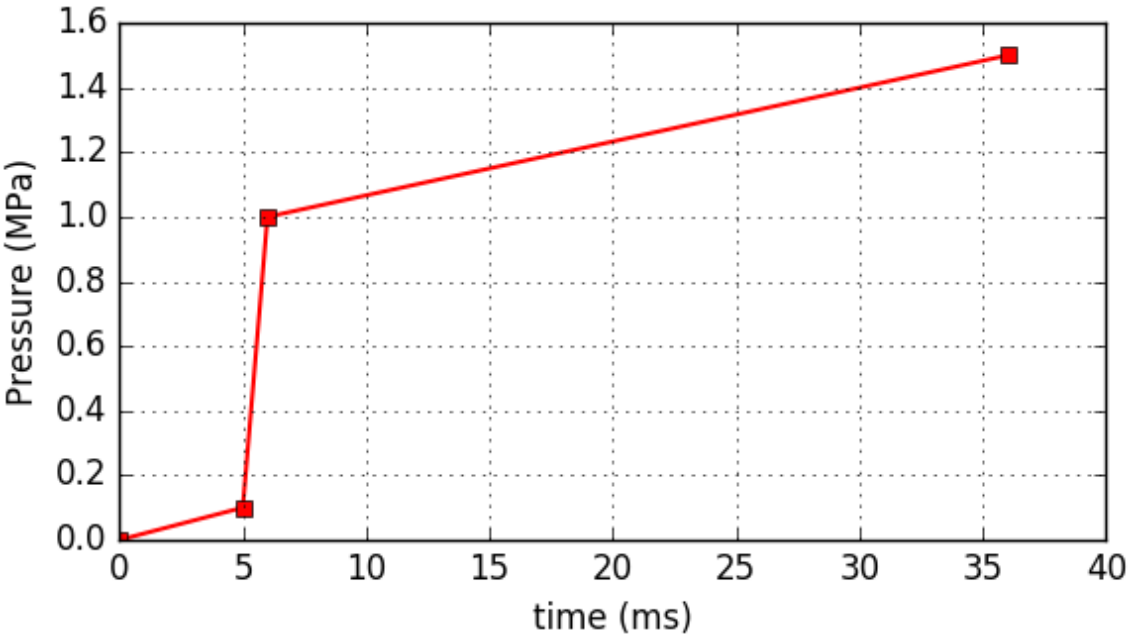

Figure 5.26: Distribution of Pressure in Simulation as per experimental data

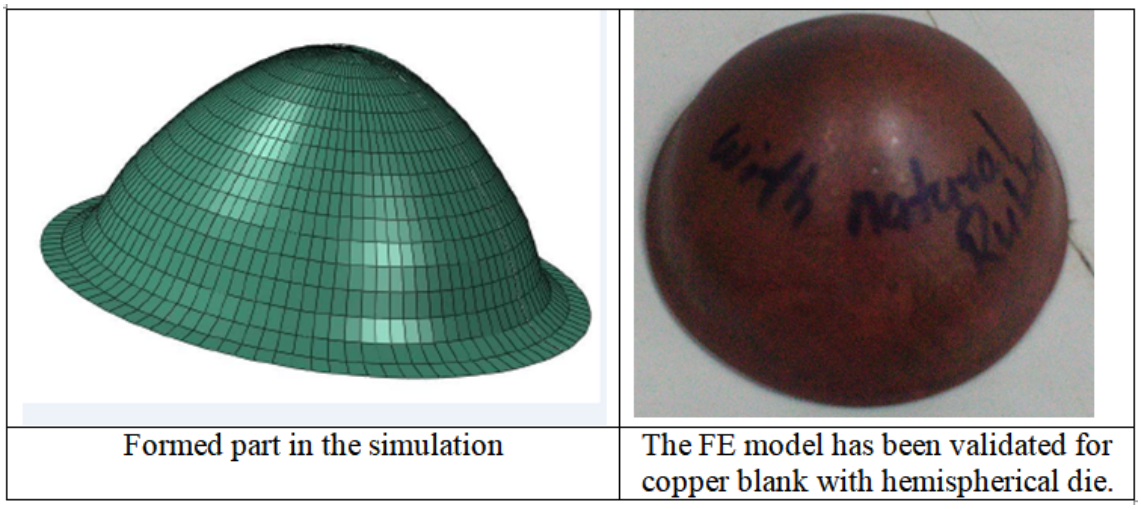

Figure 5.27: Formed cup in Simulation and actual Hardware

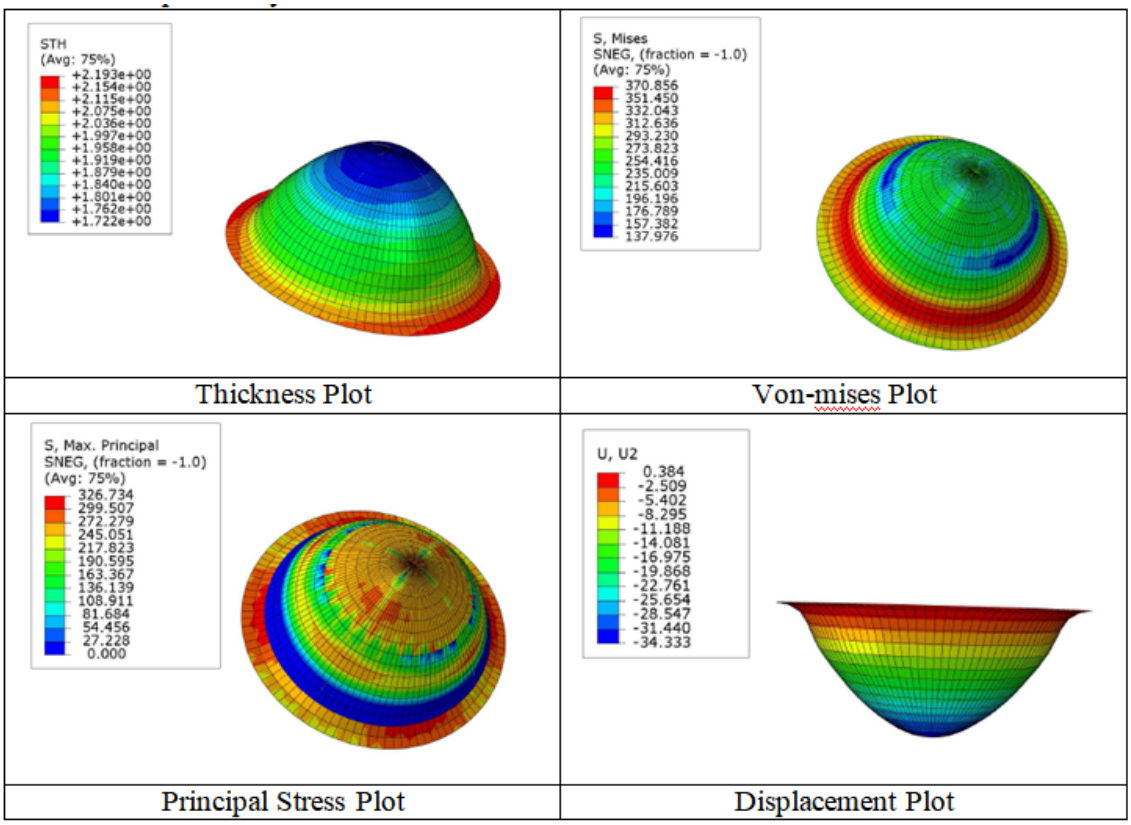

Figure 5.28: Various FEM plots

and axial deformation in the cup by applying fluid pressure is shown in figure 5.28. It is evident that by increasing fluid pressure, there exist a critical fluid pressure after which the stresses start increasing again. Optimum fluid pressure should be determined for hydro-forming process. Higher thinning at the corner reduces the possibility of the minimum corner radius that can be achieved without failure.

The plots of thickness variation, von-Mises stress variation, principal stress variation are shown in figure 5.28. The minimum wall thickness is 1.72 mm and maximum von-Mises stress is 70 MPa. The comparative plot of thickness variation is shown in figure 5.29. The thickness of the cup wall varies from 1.8mm to 2.2mm in the actual formed hemisperical cup. Whereas, in FEA simulation cup wall thickness is varying from 1.72mm to 2.2mm. The minimum thickness in both experiment and FE simulation is 1.72mm which is occuring 2mm away from the center of the cup. hence, there is a good correlation between the experiment and FE simulation.

The variation in plastic strain is shown in figure 5.30. All three processes viz. without rubber, rubber based and rubber based hydroforming are compared in terms

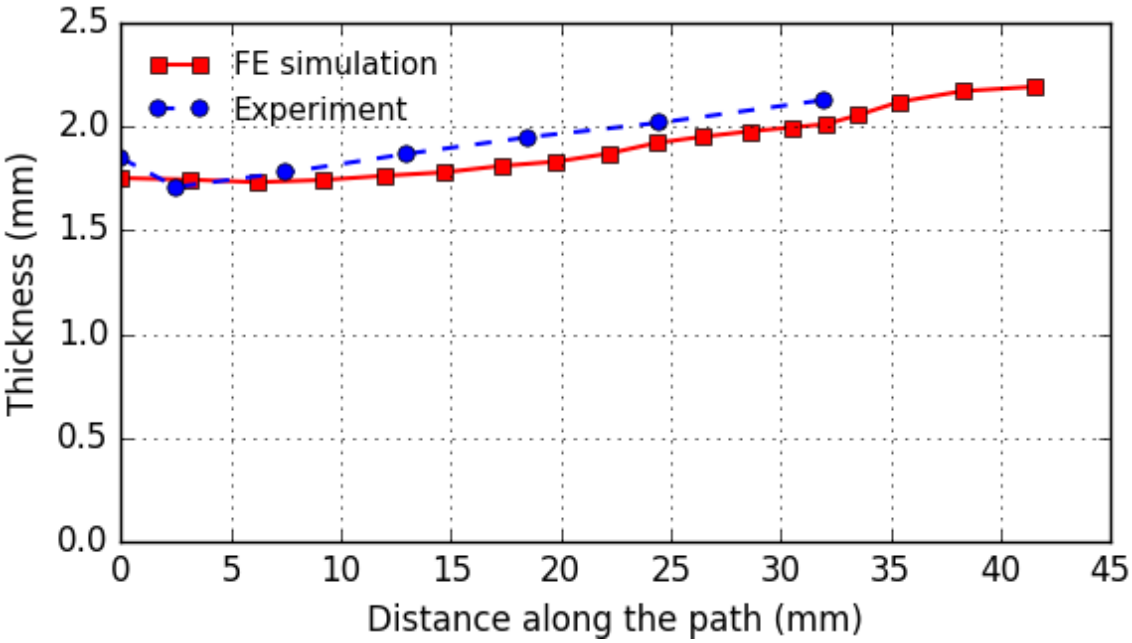

Figure 5.29: Comparison of shell thickness in simulation and experiment

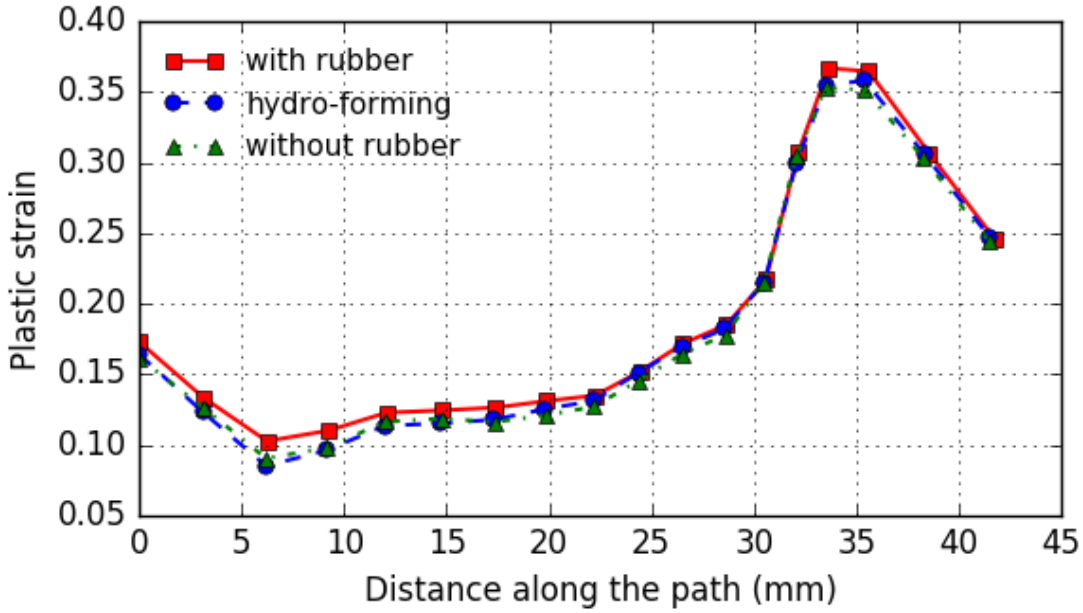

Figure 5.30: Variation of Plastic strain

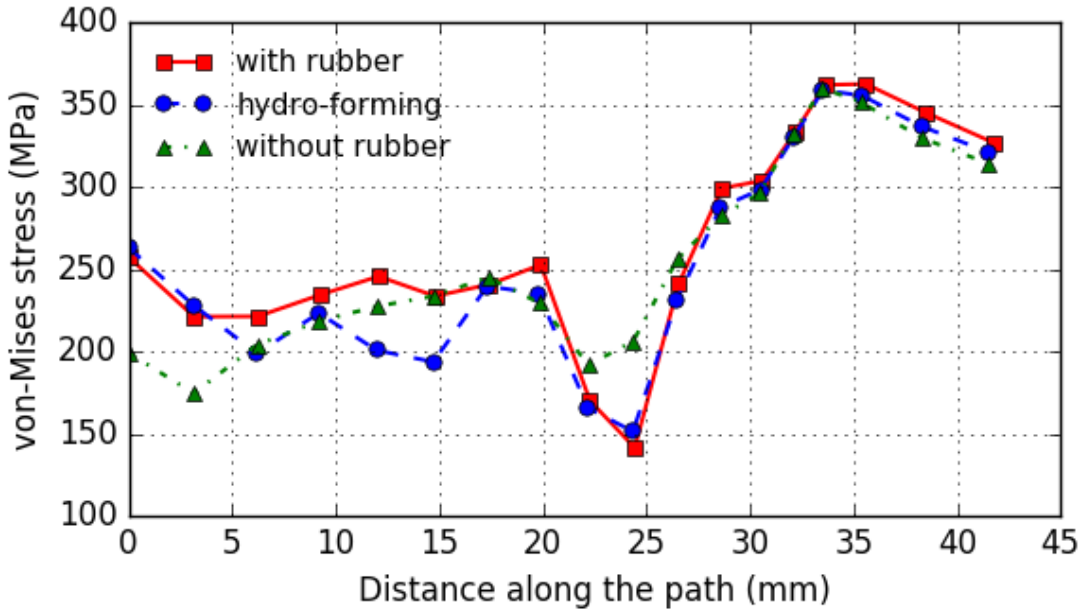

Figure 5.31: Variation of von-Mises stress

of generated plastic strain. It has been found that the maximum plastic strain is 0.36 which is occurring at the bend zone between flange and cup straight wall. The plastic strain variation is almost same in all three processes.

Figure 5.31 shows the comparative variation in von-Mises stress for all three processes. The zone of interest is the region supported by rubber which lies upto 20mm radial distance from the cup axis. In rubber based process, von-Mises stress varies between 220 MPa to 250 MPa. In rubber based hydroforming process, the variation in von-Mises stress is between 200 MPa to 250 MPa. Whereas for without rubber process, the variation in von-Mises stress is from 170 MPa to 250 MPa. Thus, it can be observed that stress distribution is uniform for rubber based forming process.

5.5 Simulation of Non-symmetric shapes using FEA

FEM analysis is also established for drawing of non-symmetric shapes in the virtual environment. The actual Material properties of Natural rubber are used here. The rubber thickness is given as 3 mm. The sheet thickness of the SS304 is 0.8 mm. The other properties are standard. The FEM model is developed using SHELL elements. Dynamic explicit analysis was carried out to get accurate results in minimum simulation time. Both elastic and plastic material properties are given in definition of Material Model. In modeling of Rubber Material actual stress-strain curve is used which is best suitable under 'Marlow Material Model' of Rubber. Dynamic explicit model is used to solve the FEM model. Punch, blank holder and die block are modeled as 'discrete rigid bodies' whereas blank and rubber are modeled as deformable bodies.

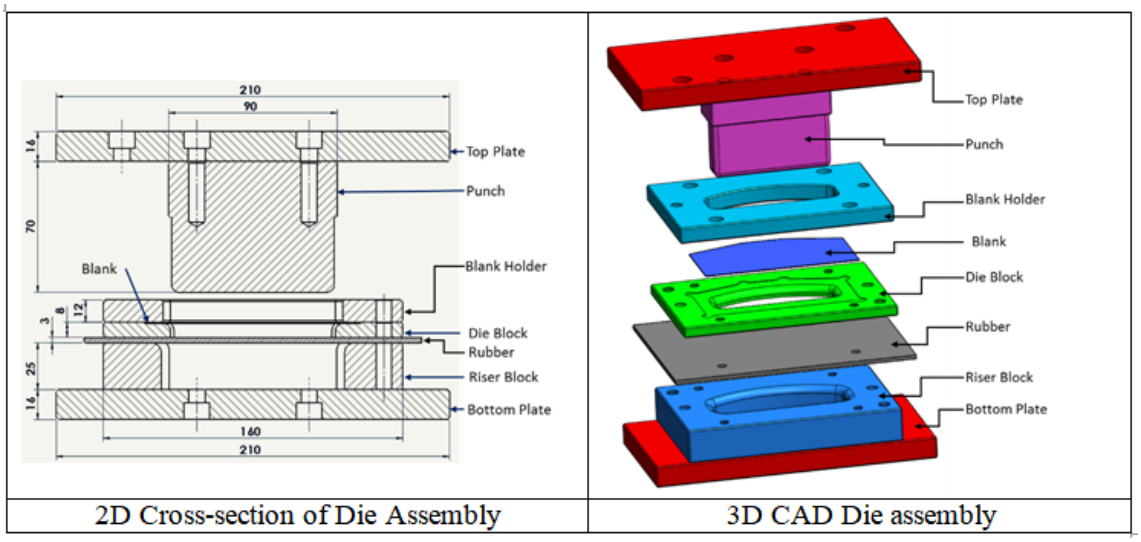

Figure 5.32: Tool Assembly for forming of Non-symmetric Component

5.5.1 Load and Boundary Conditions

Blank holder and die block are constrained in all degrees of freedom. Contact has been defined in terms of coulomb friction with friction of coefficient 0.1. The velocity of 1000mm/s is given to the punch along the forming direction. As blank is free to move in any direction, the flow of material is purely determined by friction forces acting between blank holder, die block and blank. The punch is allowed to move downward by 13.5mm. Rubber has been assigned hyper-elastic properties so

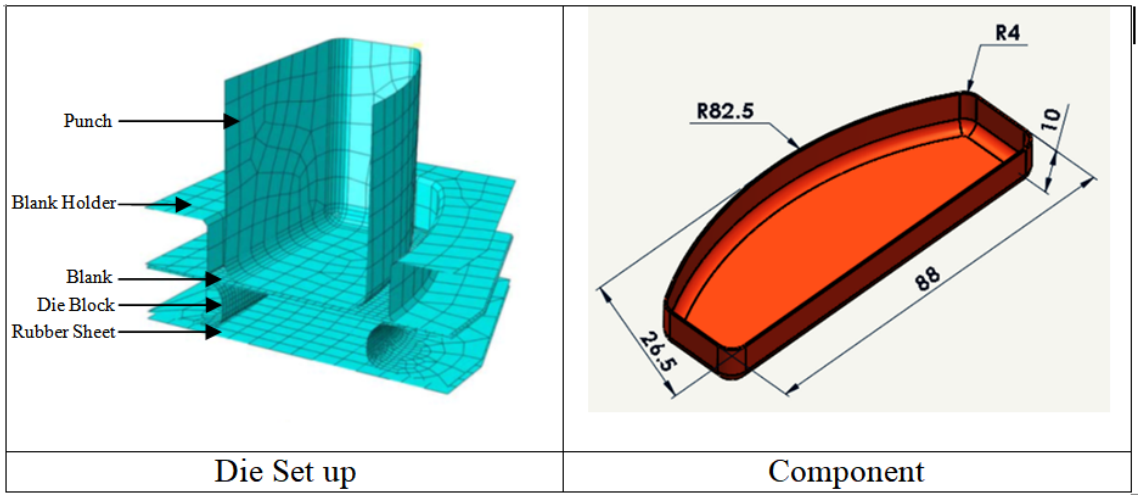

Figure 5.33: FEM model of Die assembly

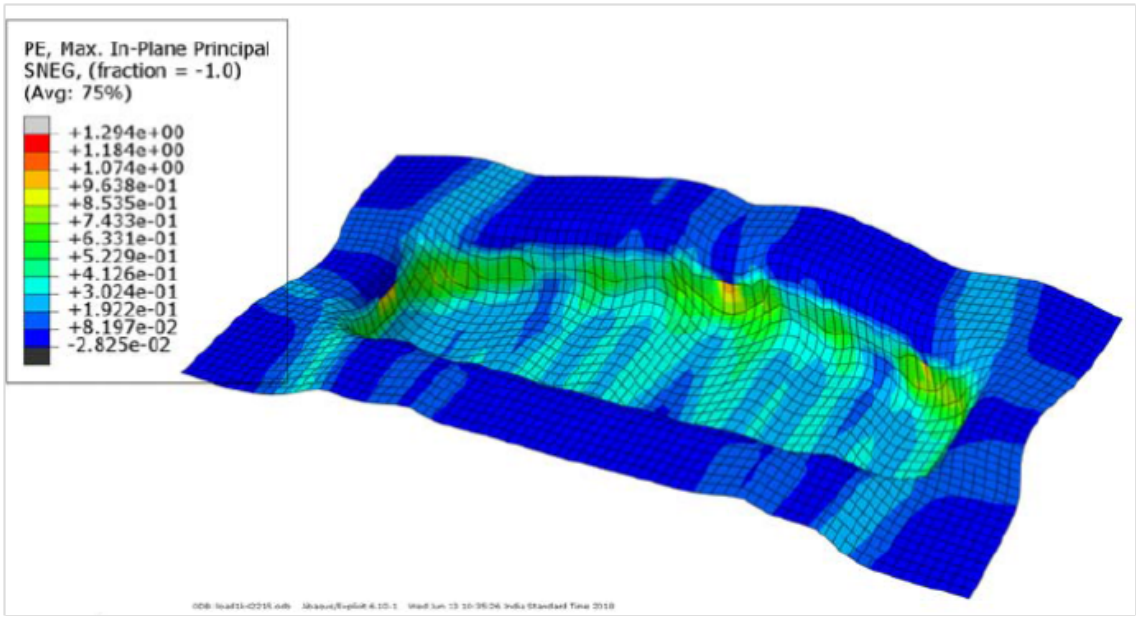

Figure 5.34: Max. Principle Stress Plot

that it expands during forming of trial component.

5.5.2 Results and Discussion

Figure 5.34 shows the maximum principle stress plot. The maximum stress observed after forming is 1294 MPa at the wall region of component. Similarly von-mises stress distribution is depicted in figure 5.35. Thickness distribution plot is shown in figure 5.36, which indicates that minimum thickness of 0.4 mm is observed at the wall region just above the base of the component. It also says that component is not failed. Figure 5.37 is showing the elastic behavior of rubber at the

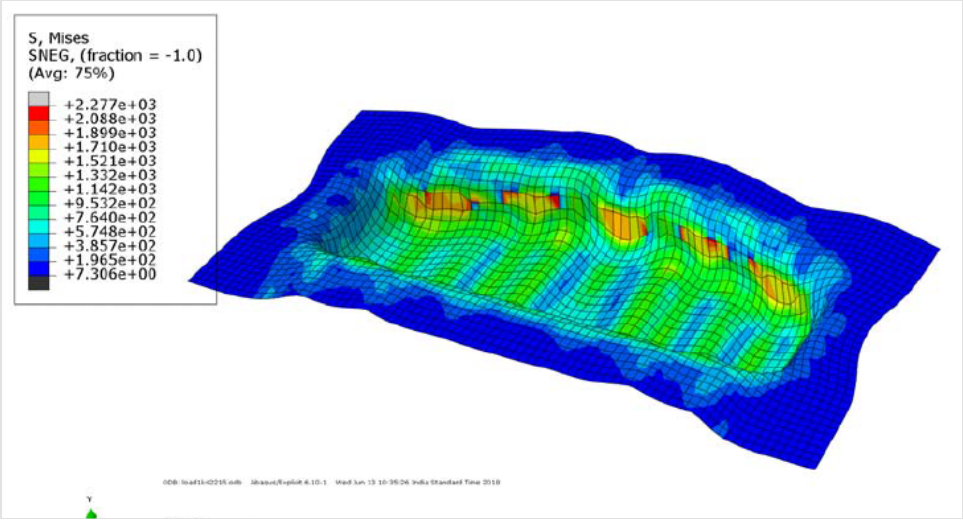

Figure 5.35: Von-Mises Plot

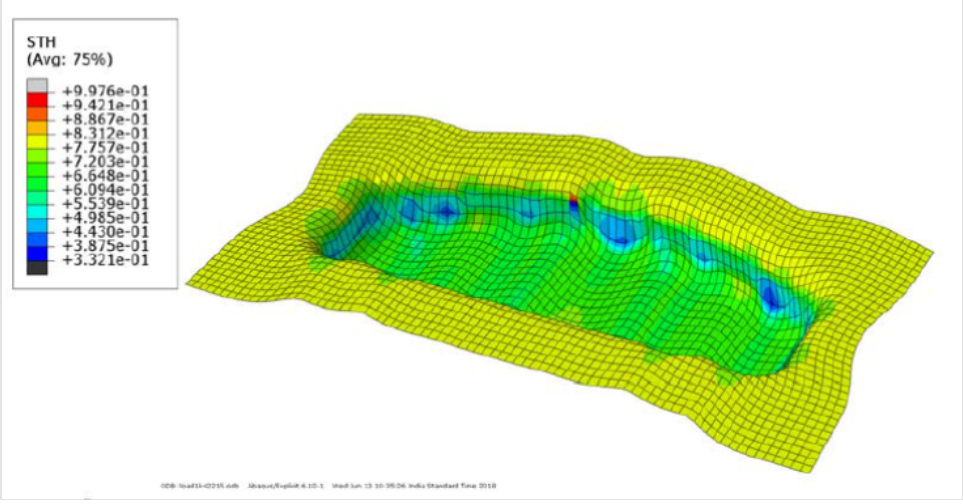

Figure 5.36: Thickness Plot

end of forming.

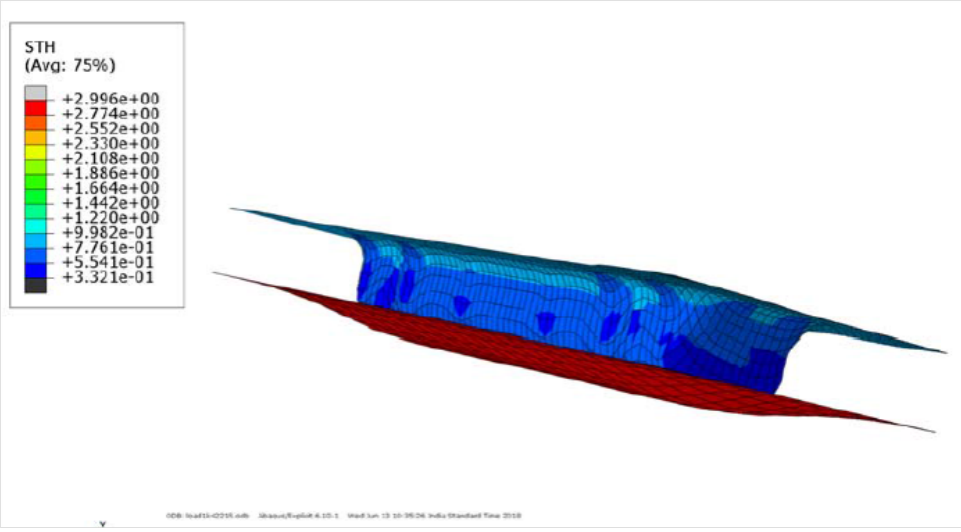

Figure 5.37: Model Showing Rubber Deformation